J Electroceram
DOI 10.1007/s10832-016-0022-5

CrossMark

The effect of ITO and Mo electrodes on the properties and stability of In-Ga-Zn-O thin film transistors

Jozeph Park[1,2] · Chang Sun Kim[3] · Yang Soo Kim[3] · Yun Chang Park[4] · Hyung Jin Park[1] · Byeong-Soo Bae[1] · Jin-Seong Park[5] · Hyun-Suk Kim[3]

Received: 16 June 2015 / Accepted: 29 February 2016
© Springer Science+Business Media New York 2016

Abstract The effect of ITO and Mo electrodes on the electrical properties and stability of In-Ga-Zn-O (IGZO) thin film transistors (TFTs) are investigated. While the field effect mobility values of the devices employing ITO and Mo electrodes are similar, the former exhibit smaller threshold voltage (V_{th}) and subthreshold swing (SS). It is suggested that the relatively large workfunction of Mo (4.7 eV) compared to that of ITO (4.4 ~ 4.5 eV) induces a large Schottky barrier at the Mo/IGZO junction, which prohibits the effective injection of electrons from the metal into the IGZO semiconductor. The workfunction of IGZO is usually reported to be approximately 4.5 eV. The device stability of the two types of TFTs under negative bias stress (NBS) and positive bias stress (PBS) is similar, which implies that the degradation of the devices under bias stress is mainly affected by the trapping of carriers at the IGZO/gate insulator interface. In the presence of illumination, the devices using optically transparent ITO electrodes allow the penetration of a more abundant concentration of photons into the IGZO active layer, and thus undergo larger V_{th} shifts under negative bias illumination stress (NBIS). However, under positive bias illumination stress (PBIS), the TFTs using ITO exhibit smaller positive V_{th} shifts. The latter phenomenon is suggested to result from the excess photo-induced electrons in the bulk that counter the effect of electron trapping near the IGZO/gate insulator boundary.

Keywords In-Ga-Zn-O (IGZO) · Thin film transistor · Negative bias stress (NBS) · Positive bias stress (PBS) · Negative bias illumination stress (NBIS) · Positive bias illumination stress (PBIS)

Jozeph Park and Chang Sun Kim contributed equally to this work.

✉ Jin-Seong Park
jsparklime@hanyang.ac.kr

✉ Hyun-Suk Kim
khs3297@cnu.ac.kr

Jozeph Park
jozeph.park@gmail.com

[1] Department of Materials Science and Engineering, KAIST, Daejeon 305-338, Republic of Korea

[2] Present address: R&D Center, Samsung Display, Yongin-Si, Giheung-Gu, Republic of Korea

[3] Department of Materials Science and Engineering, Chungnam National University, Daejeon 305-764, Republic of Korea

[4] National Nano Fab Center, Daejeon 305-806, Republic of Korea

[5] Division of Materials Science and Engineering, Hanyang University, Seoul 133-719, Republic of Korea

1 Introduction

The recent advances in the development of oxide semiconductors such as In-Ga-Zn-O (IGZO) have triggered the development of active matrix liquid crystal displays (AMLCDs) and active matrix organic light emitting diode (AMOLED) panels with more sophisticated specifications [1–3]. The relatively high electron mobility of IGZO semiconductors compared to conventional amorphous silicon (a-Si) allowed the cost-effective fabrication of high resolution displays with large dimensions [4, 5], by incorporating fast switching or driving thin film transistors (TFTs) incorporating IGZO semiconductors.

While low resistivity metals such as molybdenum (Mo), aluminum (Al), copper (Cu) and their combinations are mainly employed in the TFT arrays in order to reduce the gate signal delay over relatively large distances [6–11], the use of optically transparent electrodes is needed for the development

Published online: 02 April 2016

of next generation transparent displays. Several research groups investigated the effect of electrode materials on the properties of IGZO TFTs, however only few reports are available on their effect on device stability [11].

The present work involves a comparative study of the effect of indium tin oxide (ITO) and Mo electrodes on the properties and stability of IGZO devices. The relatively large workfunction of Mo compared to that of ITO is suggested to induce a high Schottky barrier at the Mo/IGZO boundary, which results in larger threshold voltage (V_{th}) and subthreshold swing (SS) values. While the initial transfer characteristics are different, the device stability under negative bias stress (NBS) and positive bias stress (PBS) is not affected by the electrode material. This is indicative of charge trapping at the IGZO/gate insulator being the major degradation mechanism. In the presence of visible light, the transparent ITO allows the penetration of photons into the active layer more abundantly, and thus the device stability under negative bias illumination stress (NBIS) is more pronounced as compared with the devices using Mo electrodes. Under positive bias illumination stress (PBIS), the TFTs using ITO electrodes undergo smaller degradation, which is conjectured to occur by the excess photo-induced electrons in the semiconductor bulk to have a counter effect on the tendency of the V_{th} to shift towards positive values.

2 Experimental procedure

IGZO films with a 50 nm thickness were grown onto glass substrates by radio-frequency (RF) sputtering. A target with a In:Ga:Zn atomic ratio of 1:1:1 was used, and the RF power was 100 W. The deposition was done under a working pressure of 5 mTorr, with a Ar/O_2 gas ratio of 50:1 sccm. The optical transmittance of IGZO on glass was measured using a UV–vis spectrometer, and the microstructure was examined by X-ray diffraction (XRD). The optical bandgap of IGZO was estimated by fitting a Tauc plot from optical UV–vis optical transmittance. Atomic force microscopy (AFM) was performed to examine the surface roughness of the IGZO layer. Transmission electron microscopy (TEM) investigations were performed using a JEOL JEM-ARM200F electron microscope operating at 200 kV. Energy dispersive X-ray spectroscopy (EDS) analyses were carried out using a beam

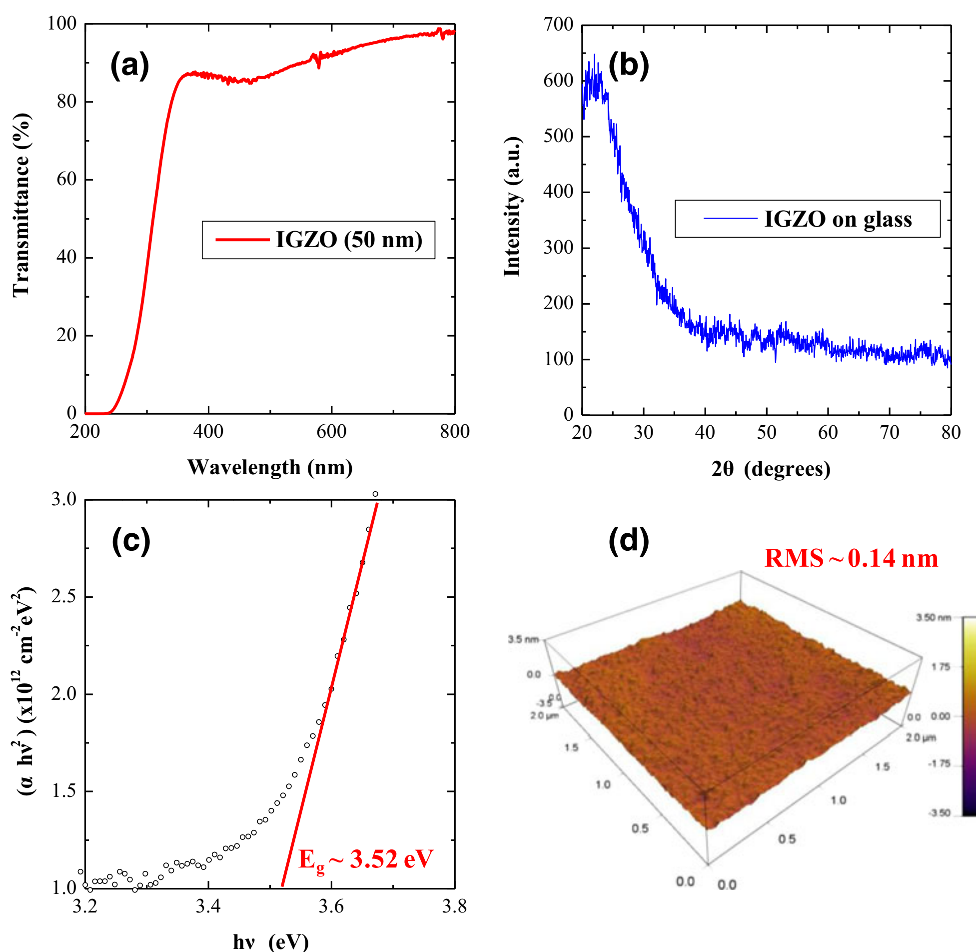

Fig. 1 (**a**) UV–vis optical transmittance of 50 nm-thick IGZO, which was normalized with respect to the transmittance of the glass substrate. (**b**) X-ray diffractograms of IGZO on glass, indicating an amorphous microstructure. (**c**) Tauc plot of IGZO using optical UV–vis optical transmittance. (**d**) AFM profile of IGZO surface

size of 1 nm in scanning TEM (STEM) mode to obtain elemental maps.

TFT devices were fabricated on highly doped p-type Si substrates with a thermally grown 100 nm-thick SiO_x. The latter is used as the gate insulator. 50 nm-thick IGZO films were grown onto the Si/SiO_x substrates, and patterned with shadow masks to form the active islands. Next, two types of electrode materials were sputter-deposited, namely indium tin oxide (ITO) and molybdenum (Mo) with 40 nm and 40 nm thickness, respectively. The source-drain electrodes were formed by shadow masks. The final devices were each annealed at 250 °C for 1 h.

The electrical properties of the TFTs were evaluated using a Keithley parameter analyzer, including the initial transfer curves and output characteristics. The devices were then subjected to gate bias stress under different conditions; negative bias stress (NBS), negative bias illumination stress (NBIS) with a top light source of 1500 lux illuminance, positive bias stress (PBS) and positive bias illumination stress (PBIS), also with a 1500 lux light source. The gate voltage (V_g) and dra in voltage (V_d) applied during negative bias stress were −20 V and +5 V, respectively. The V_g and V_d values for positive bias stress were +20 V and +5 V, respectively. Each stress experiment was conducted at room temperature for a total time of 1 h.

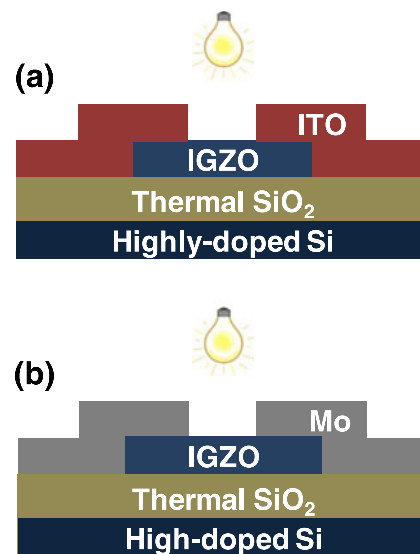

Fig. 2 Schematic cross sectional diagram of the TFT devices using (**a**) ITO and (**b**) Mo electrodes

3 Results and discussions

Figure 1 shows the optical transmittance, XRD diffractograms, optical bandgap, and AFM roughness results of IGZO on glass. The average optical transmittance of the 50 nm-thick IGZO over the visible range of the

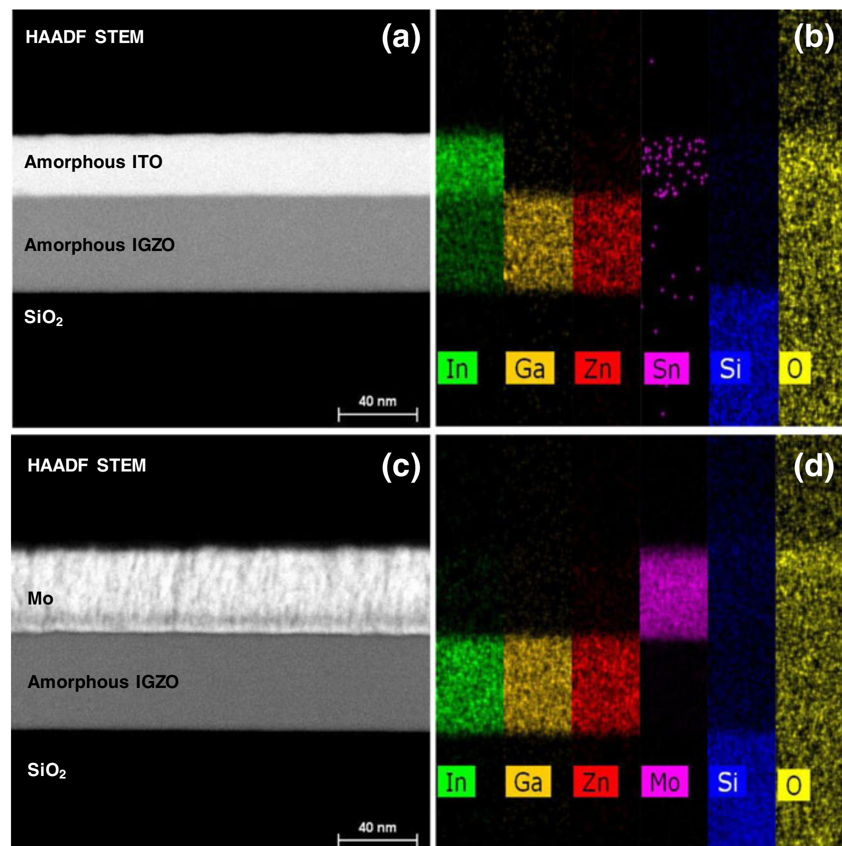

Fig. 3 Cross-sectional scanning transmission electron microscopy (STEM) images collected using a high-angle annular dark-field (HAADF) detector. (**a**) IGZO TFT with ITO electrodes. (**b**) Elemental mappings in the scanned region of (**a**). (**c**) IGZO TFT with Mo electrodes. (**d**) Elemental mapping in the scanned region of (**c**)

electromagnetic spectrum (400 ~ 700 nm) is approximately 90.1 % (Fig. 1(a)). The XRD pattern does not display any particular crystallographic peak, which indicates that the IGZO film grown in this work is amorphous (Fig. 1(b)). The optical bandgap of IGZO was determined by plotting the absorption coefficient with respect to photon energy. A bandgap energy of approximately 3.52 eV was extracted by extrapolating the linear region of the absorption coefficient (Fig. 1(c)). AFM results indicate a relatively small root mean square (RMS) roughness value of approximately 0.18 nm, which suggests again that IGZO was grown with a uniform, amorphous structure.

Figure 2 shows the schematic diagram of the TFT devices using ITO and Mo electrodes. Here, the highly doped Si substrate is used as the gate electrode. The light source is placed above the devices, so the transparent ITO allows the effective illumination of a larger portion of the IGZO islands as compared to the devices using opaque Mo metal.

Figure 3 consists of cross-sectional scanning high angle annular dark field transmission electron microscopy (TEM) images of the TFTs and the elemental distribution in the scanned region by energy dispersive X-ray spectroscopy (EDS). Clear elemental signals of the constituent layers confirm the formation of IGZO and the physical interface between the semiconductor and the Mo or ITO electrodes.

The transfer curves showing the drain current (I_d) with respect to V_g and output characteristics (I_d vs. V_d) of the devices using ITO and Mo electrodes are shown in Fig. 4. The representative parameters such as field effect mobility (μ_{FE}), threshold voltage (V_{th}) and subthreshold swing (SS) are listed in Table 1. Because the devices with Mo electrodes exhibit more positive V_{th} values, the I_d levels at a given gate voltage are smaller than those using ITO electrodes. Hard saturation occurs at V_d values greater than 5 V at $V_g = 10$ V, which indicate that the devices function well with sufficient pinch-off occurring near the drain junction.

While the μ_{FE} values are similar, the difference in V_{th} and SS between the devices using ITO and Mo electrodes may originate from the different workfunctions of the two electrode materials. The workfunction of IGZO is usually reported to be approximately 4.5 eV [12]. Here, the relatively large workfunction of Mo (4.7 eV) [13] compared to that of ITO (4.4 ~ 4.5 eV) [14] may be expected to induce a large Schottky barrier at the Mo/IGZO junction, which prohibits the effective injection of electrons from

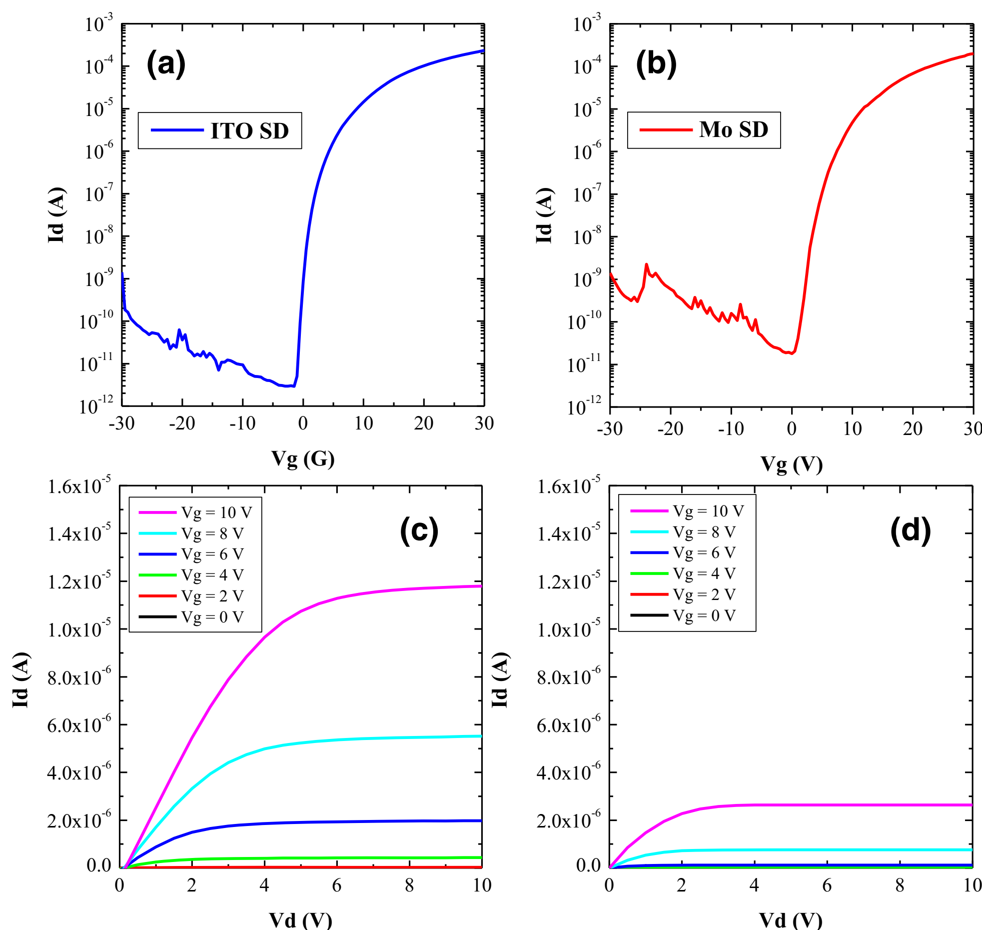

Fig. 4 Transfer curves of the TFT devices using (**a**) ITO and (**b**) Mo electrodes. Output haracteristics of the TFT devices using (**c**) ITO and (**d**) Mo electrodes

Table 1 Representative electrical parameters of the IGZO TFTs using ITO and Mo electrodes, extracted from the transfer curves

Electrode	μ_{FE} (cm^2/Vs)	V_{th} (V)	SS (V/dec)
ITO	6.17 ± 0.15	4.53 ± 0.20	0.40 ± 0.30
Mo	6.22 ± 0.47	7.33 ± 0.24	0.69 ± 0.13

Table 2 ΔV_{th} values of the IGZO TFTs using ITO and Mo electrodes, under NBS, NBIS, PBS and PBIS

Electrode	NBS	NBIS	PBS	PBIS
ITO	−0.52 ± 0.23	−4.89 ± 0.47	8.20 ± 0.63	4.53 ± 0.42
Mo	−0.65 ± 0.19	−1.46 ± 0.28	8.23 ± 0.57	5.89 ± 0.36

the metal into the IGZO semiconductor. On the other hand, the ITO/IGZO junction may be anticipated to exhibit a comparatively Ohmic behavior. Therefore, a relatively slow increase in I_d occurs with respect to the applied V_g in the devices using Mo electrodes, hence the more positive V_{th} and larger SS values.

The devices were then subjected to bias stress experiments, and the amount of V_{th} shift (ΔV_{th}) was evaluated for each TFT after 1 h of stress time. For each stress condition, a total of 4 devices were tested, and the results are plotted in Fig. 5. The total ΔV_{th} values are listed in Table 2.

Note that the amount of degradation under NBS and PBS in the dark state is of the same magnitude for the devices using ITO and Mo electrodes. Since IGZO is a typical n-type semiconductor, negligible concentrations of hole carriers are present, thus negligible charge trapping occurs at the IGZO/SiO_x interface under NBS conditions [15]. On the other hand, under PBS, the trapping of major electron carriers at the IGZO/SiO_x interface is well known to induce positive V_{th} shifts [16], which is the case for the IGZO devices in this work.

In the presence of light, a number of degradation mechanisms under NBIS is available in the literature, including the trapping of photo-induced holes at the IGZO/gate insulator interface [17–19], the release of excess free electrons by the ionization of oxygen vacancies ($V_O + h\nu \rightarrow V_O^{2+} + 2e^-$) [20, 21] or by the formation of peroxides ($O^{2-} + O^{2-} \rightarrow O_2^{2-} + 2e^-$) [22]. The latter mechanisms have been attracting attention recently, as they provided reasonable explanations for a physical phenomenon called persistent photoconduction (PPC). According to several studies on PPC, once electron–hole pairs are formed, the holes become localized at sub-gap defect levels and do not recombine easily with electrons. The dissociation of electrons and holes thus contribute excess free carriers in oxide semiconductors, and induce negative V_{th} shifts [23].

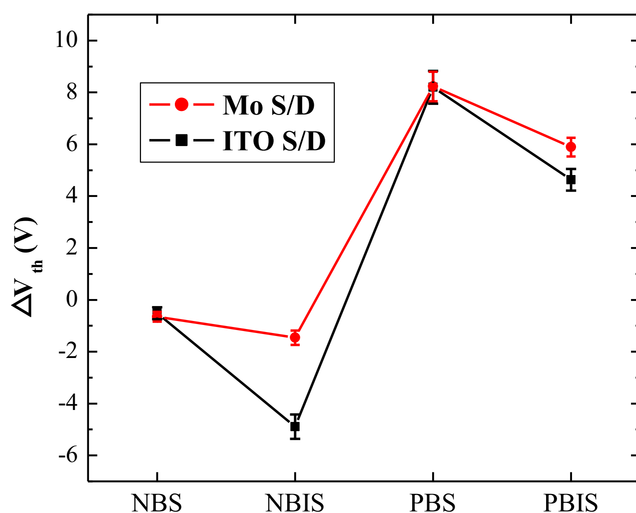

Fig. 5 ΔV_{th} values of the IGZO devices using ITO and Mo electrodes under NBS, NBIS, PBS and PBIS conditions

For the devices using ITO electrodes, the larger V_{th} shifts compared to those using Mo electrodes are most likely to result from the optical transparency of ITO. A larger area of the IGZO semiconductor under ITO electrodes and consequently more excess electrons are released by the interaction of oxygen anions and photons, as compared with the devices using opaque Mo electrodes. The relatively large concentration of excess electrons is thus expected to induce relatively large negative V_{th} shifts in the devices with ITO electrodes during NBIS.

Under PBIS, both devices exhibit smaller V_{th} shifts than under PBS. In this case, it may be anticipated that the photo-induced excess electrons have a counter effect on the tendency of the V_{th} to shift towards positive values. Therefore, two competing mechanisms are present in this case. One acts as a driving force that induces negative V_{th} shifts by the release of excess free electrons as a result of photon radiation. The other driving force simply consists of electron trapping at the IGZO/SiO_x interface by the positive gate bias. The devices using ITO electrodes undergo smaller V_{th} shifts than the ones using Mo electrodes, again because of their transparency, allowing excess photo-induced electrons in the semiconductor bulk to counter the effect of electron trapping near the IGZO/gate insulator boundary.

When illuminated, the ITO/IGZO interface is not expected to play a major role in the device degradation by either NBIS or PBIS. For example, if any charges were to be trapped at the ITO/IGZO junction, the negative gate bias during NBIS would induce electron trapping at the ITO/IGZO interface. If this were true, the trapped electrons would screen the gate voltage during the transfer curve sweep, and impede the effective charge injection from the source electrode into the semiconductor. This would make the V_{th} shift towards positive values. The opposite is observed in the experimental results, therefore the ITO/IGZO interface may be neglected. By the same principle, the positive gate bias during PBIS

would induce net positive charge trapped near the ITO/IGZO interface. If this were true, the trapped positive charge would attract electrons from the source electrode into the semiconductor during the transfer curve sweep, and make the Vth shift towards negative values.

The above results indicate that in order to fabricate transparent TFTs using transparent electrodes, an effective way to shield the semiconductor layer from external light must be devised. If the gate electrodes are also transparent, the use of an opaque light shield that covers the active island both on top and bottom shall be necessary, so as to minimize device degradation under NBIS or PBIS.

4 Conclusion

The effect of ITO and Mo source-drain electrodes was studied in IGZO TFTs. While the field effect mobility values of the two devices are similar, the devices using Mo exhibit more positive V_{th} and larger subthreshold swing values. The latter is anticipated to occur owing to the larger workfunction of Mo (~4.7 eV) than that of ITO (4.4~4.5 eV), which forms a larger Schottky barrier in contact with IGZO, of which the workfunction is usually known to be approximately 4.5 eV.

The devices using ITO and Mo electrodes exhibit similar V_{th} shifts under NBS and PBS without illumination. It is reasonable to conclude that the major degradation originates from charge being trapped at the IGZO/gate insulator interface. In the presence of light, the TFTs using ITO electrodes undergo larger V_{th} shifts in the negative direction under NBIS than those using Mo, due to the larger number of photons reaching the IGZO through the transparent ITO. For PBIS tests, both types of devices undergo smaller V_{th} shifts in the positive direction than under PBS. It is suggested that excess photo-induced electrons counter the total positive V_{th} shift that would occur under PBS. This effect is more pronounced in the devices using transparent ITO electrodes, where a larger area of IGZO under the electrode is exposed to photon radiation, compared to those using opaque Mo electrodes.

Acknowledgments This work was supported by Basic Science Research Program through the National Research Foundation of Korea (NRF) funded by the Ministry of Education (Grant No: 2014R1A1A2055138).

References

1. K. Nomura, H. Ohta, A. Takagi, T. Kamiya, M. Hirano, H. Hosono, Nature **432**, 488 (2004)
2. J.S. Park, W.J. Maeng, H.S. Kim, J.S. Park, Thin Solid Films **520**, 1679 (2012)
3. J.S. Park, H. Kim, I.D. Kim, J. Electroceram. **32**, 117 (2014)
4. H. Hosono, J. Non-Cryst. Solids **352**, 851 (2006)
5. M.J. Powell, IEEE Trans. Electron. Dev. **36**, 12 (1989)
6. T. Mudgal, N. Walsh, R.G. Manley, K.D. Hirschman, ECS J. Solid State Sci. Technol. **3**, Q3032 (2014)
7. K.H. Choi, H.K. Kim, Appl. Phys. Lett. **102**, 052103 (2013)
8. P. Barquinha, A.M. Vilà, G. Gonçalves, L. Pereira, R. Martins, J.R. Morante, E. Fortunato, IEEE Trans. Electron. Dev. **55**, 4 (2008)
9. K. Park, J.Y. Choi, H.J. Lee, J.Y. Kwon, H.S. Kim, Jpn. J. Appl. Phys. **50**, 096504 (2011)
10. A. Kiani, D.G. Hasko, W.I. Milne, A.J. Flewitt, Appl. Phys. Lett. **102**, 152102 (2013)
11. M. Nag, A. Bhoolokam, S. Steudel, A. Chasin, G. Groeseneken, P. Heremans, J. Soc. Inf. Disp. **22**(6), 310–315 (2014)
12. T.C. Fung, C.S. Chuang, C. Chen, K. Abe, R. Cottle, M. Townsend, H. Kumomi, J. Kanicki, J. Appl. Phys. **106**, 084511 (2009)
13. S. Berg, P.O. Gartland, B.J. Slagsvold, Surf. Sci. **43**, 275 (1974)
14. K. Sugiyama, H. Ishii, Y. Ouchi, K. Seki, J. Appl. Phys. **87**, 295 (2000)
15. K.S. Jang, J. Raja, J.W. Kim, C.M. Park, Y.J. Lee, J.H. Yang, H.S. Kim, J.S. Yi, Semicond. Sci. Technol. **28**, 085015 (2013)
16. T.C. Chen, T.C. Chang, T.Y. Hsieh, W.S. Lu, F.Y. Jian, C.T. Tsai, S.Y. Huang, C.-S. Lin, Appl. Phys. Lett. **99**, 022104 (2011)
17. K.H. Lee, J.S. Jung, K.S. Son, J.S. Park, T.S. Kim, R. Choi, J.K. Jeong, J.Y. Kwon, B.W. Koo, S.Y. Lee, Appl. Phys. Lett. **95**, 232106 (2009)
18. J.H. Shin, J.S. Lee, C.S. Hwang, S.H.K. Park, W.S. Cheong, M.K. Ryu, C.W. Byun, J.I. Lee, H.Y. Chu, ETRI J. **31**, 1 (2009)
19. J.H. Jeon, J.H. Kim, M.K. Ryu, J. Korean Phys. Soc. **58**, 158 (2011)
20. K. Ghaffarzadeh, A. Nathan, J. Robertson, S.W. Kim, S.H. Jeon, C.J. Kim, U.I. Chung, J.H. Lee, Appl. Phys. Lett. **97**, 113504 (2010)
21. B.K. Ryu, H.K. Noh, E.A. Choi, K.J. Chang, Appl. Phys. Lett. **97**, 022108 (2010)
22. H.H. Nahm, Y.S. Kim, D.H. Kim, Phys. Status Solidi B **249**, 1277 (2012)
23. S.H. Jeon, S.E. Ahn, I.H. Song, C.J. Kim, U.I. Chung, E.H. Lee, I.K. Yoo, A. Nathan, S.S. Lee, K. Ghaffarzadeh, J. Robertson, K.N. Kim, Nat. Mater. **11**, 301 (2012)